

Near-Infrared Absorption in Symmetric Squarylium and Croconate Dyes: A Comparative Study Using Symmetry-Adapted Cluster-Configuration Interaction Methods

Ch. Prabhakar,^{†,‡} K. Yesudas,[†] G. Krishna Chaitanya,[†] Sanyasi Sitha,[†]
K. Bhanuprakash,^{*,†} and V. Jayathirtha Rao^{*,‡}

Inorganic Chemistry Division and Organic Chemistry Division, Indian Institute of Chemical Technology, Hyderabad-500 007, India

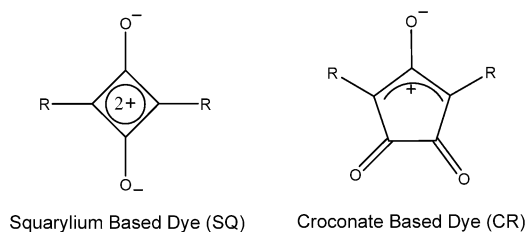
Received: March 30, 2005; In Final Form: July 11, 2005

Symmetric croconate (CR) and squarylium dyes (SQ) are well-known near-infrared (NIR) dyes and, in general, are considered to be donor–acceptor–donor type molecules. It is established in the literature that CR dyes absorb in a longer wavelength region than the corresponding SQ dyes. This has been attributed to the CR ring being a better acceptor than the SQ ring. Thus increasing the donor capacity should lead to a bathochromic shift in both SQ and CR. On the other hand, some experiments reported in the literature have revealed that increasing the conjugation in the donor part of the SQ molecule leads first to red shift, which upon a further increase of the conjugation changes to a blue shift. Hence, to understand the role of the central ring and the substitutions in the absorption of these dyes, we carried out high-level symmetry-adapted cluster-configuration interaction (SAC–CI) calculations of some substituted SQ and CR dyes and compare the absorption energy with the existing experimental data. We found that there is very good agreement. We also carried out SAC–CI calculations of some smaller model molecules, which contain the main oxyallyl substructure. We varied the geometry (angle) of the oxyallyl subgroup and the substitution in these model molecules to establish a correlation with the bathochromic shift. We found that the charge transfer is very small and does not play the key role in the red shift, but on the other hand, the perturbation of the HOMO–LUMO gap (HLG) from both the geometry and substitution seems to be responsible for this shift. We suggest as a design principle that increasing the donor capacity of the groups may not help in the red shift, but introducing groups which perturb the HLG and decrease it without changing the MO character should lead to a larger bathochromic shift.

Introduction

“Functional” dyes are of current research interest as they have applications in optical devices, such as optical switches and saturable absorptive mirrors, and as materials in electrophotographic reproduction, solar cells, etc.^{1–4} Of particular interest are the organic functional dyes because they have features such as flexibility, a high interaction with light, and most important, the ability to custom tailor the synthesis of the dye in an absorption range of choice. Here, computational chemistry based on quantum chemical theories, which are replacing the earlier empirical rules, is playing a major role in understanding the dyes post priori experiment or in suggesting modifications for the a priori synthesis suitable to the applications.^{1–2} Recent studies of the organic dyes have concentrated in the absorption range greater than 1000 nm, as these are useful in telecommunication-based optical devices, in medicine, semiconductor lasers, etc.^{5–7} Because they absorb in the near-infrared region, these dyes are also referred to as NIR dyes.¹ Some promising NIR dyes are the squarylium (SQ) dyes (Scheme 1), croconate (CR) dyes (Scheme 1), and the recently synthesized derivatives of di-(benzofuranonyl)methanolate (BM dye), all of which contain the meso-ionic oxyallyl substructure.^{1,5} We have very recently carried out symmetry-adapted cluster-configuration

SCHEME 1: Representative Structures for Squarylium- and Croconate-Based Dyes



interaction (SAC–CI) studies of the BM dye and attributed the large red shift to orbital interactions.⁸

The symmetric SQ and CR dye derivatives in general have been classified as donor–acceptor–donor (D–A–D) type molecules.^{3,9–13} It has been suggested that the reason SQ dyes in general absorb at lower wavelengths of at least 100 nm when compared to the CR dyes is because the SQ ring is a weaker acceptor than the CR ring.⁹ One of the earliest calculations of a SQ derivative has been reported by Bigelow and Freund who assumed a D–A–D type character and carried out modified neglect of differential overlap (MNDO) and complete neglect of differential overlap/spectroscopic (CNDO/s) (single and double energy selected configuration interaction) calculations and arrived at the conclusion that the singlet–singlet transition (S_0 – S_1) has a large oscillator strength because of the HOMO–LUMO orbital delocalization over the backbone and that the amino group nitrogen donates very little charge. On the other

* To whom correspondence should be addressed. E-mail: bhanu2505@yahoo.co.in.

[†] Inorganic Chemistry Division.

[‡] Organic Chemistry Division.

hand, the oxygen atoms act as acceptors in the ground state and as donors in the excited state, which inhibits the charge transfer.¹⁴ The major conclusion is that these are π - π^* transitions occurring at the center of the molecule (i.e., the squaraine moiety). Studies by Law on the structural changes on absorption in squaraine dye derivatives showed that there is very little shift of the absorption band upon substitution and changing of the solvents.¹³ This has been attributed to the noninvolvement of the donor group in the S_0 - S_1 excitation.^{3,13} Law also points out that in accordance with the calculations of Bigelow and Freund, though these are primarily charge-transfer states, the bathochromic shift, induced by changing the substitutions, is very small when compared to other polar molecules.³ Langhals recently analyzed the reason for the drastic red shift in the BM dye;⁹ it was suggested that the carbenium ion is the acceptor and, on the basis of the König and Ismailsky empirical model of $D-\pi-A-\pi-D$,¹⁵⁻²¹ absorbs in the longer wavelength region because of the increased π conjugation. When this acceptor is replaced by squaric acid, which contains two formal positive charges, the absorption shifts to the red, and when the squaric acid is replaced by the croconic acid, which is supposed to contain three positive charges, a larger red shift is seen. Meier et al. suggested that the oxyallyl substructure-based central ring is the acceptor, to red shift the absorption, the π conjugation in the donor region has to be extended.¹⁰⁻¹¹ But in another recently reported experiment by the same group on the effect of increasing the conjugation using stilbenoid moieties on the squaraines (1,3-substituted), they observed that there was first a bathochromic shift of around 300 nm and that a further increase of the conjugation results in a hypsochromic shift of around 200 nm in contrast to the normal conjugated oligomers which show a convergence of the absorption.¹² They concluded that this influence of the stilbene building moieties is not in line with the quantum chemical treatment of the squaraines carried out by Bigelow and Freund, where it has been suggested that the entire charge localizes on the central ring.¹⁴ Simard et al. recently synthesized chalcogenopyrylium derivatives of SQ and CR dyes and compared their absorption properties using spectroscopic techniques.²² They observed that as the heteroatoms in the ring become larger the absorption maximum moves to longer wavelengths. They also observed that the CR dyes always had a longer absorption by 130–170 nm. The oxidation–reduction potentials, measured with the cyclic voltammeter for two representative dyes from both the SQ and CR series, suggest that the differences in absorption is LUMO driven rather than HOMO driven. As a consequence, they concluded that the HOMO–LUMO gap (HLG) is basically the result of the change in LUMO levels.²²⁻²³

On the basis of the observations reported above, some questions that crop up are (1) are these typical $D-A-D$ molecules, (2) is CR a better acceptor than SQ because it has more carbonyl groups and is this the reason for showing the bathochromic shift, and (3) is there a substantial charge transfer between the donors and the ring. In a continuation of our earlier studies of such type of dyes⁸ we have carried out detailed studies here first on some model molecules, which should illuminate the behavior of the oxyallyl substructure, and then we extended the study to the larger molecules to answer the questions raised above. We have come across only one study where the Pariser–Parr–Pople (PPP) methodology was used to study these two dyes.²⁴ Their main conclusion was that the CR dyes absorb around 100 nm in the longer wavelength, but no detailed explanation was offered for this behavior. Other than these, most of the theoretical studies concentrated only on the SQ dyes.²⁴⁻³⁰

To the best of our knowledge, there are no high-level theoretical studies comparing these two moieties in terms of the acceptance capacity of the ring and the charge transfer in the dye.

Computational Details

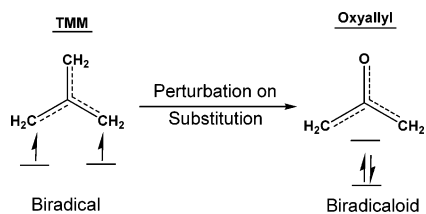
SAC–CI methods have been applied for many molecules and found to be quite accurate for studying molecular spectroscopy.³¹⁻³⁵ Basically, the SAC–CI is a cluster expansion method, and it is usually more rapidly convergent than CI. SAC–CI methods take into consideration the singly and doubly excited states which mix up with the ground state and the targeted excited state. More details of this method are available in the literature.³¹⁻³⁵ We had applied this technique in our previous study of dyes based on the oxyallyl substructure with success (a difference of less than 0.1 eV from the experimental observed excitation energy was obtained); therefore, it is our choice for this study also.⁸ In similar lines to our earlier study and earlier reports by other researchers, the geometry of all the molecules in this work also have been optimized using DFT methods and then subjected to SAC–CI.^{8,36}

We used the B3LYP hybrid functional and a 6-31G(d,p) basis set to determine the geometry with the built-in ab initio software, G03W.³⁷ We optimized both the lowest-singlet and triplet states for the SQ and CR derivatives. We found that the singlet states are of lower energy. The vibrational analysis was carried out to ensure that there are no negative frequencies and hence confirmed the minima on the potential energy surface. The singlet geometries thus obtained were then subjected to SAC/SAC–CI calculations to study the singlet–singlet transition using G03W.³⁷ For the ground state, SAC was carried out with nonvariational methods, while for the excited state, SAC–CI was carried out using variational methods. The active space was chosen with a window option where, depending on the molecule's size, some core and some virtual molecular orbitals are not used in the active space (the minimum is not less than 160 orbitals and the maximum is 216 orbitals). In most of the small molecules, the entire active space is used. For the ground state, all of the single-excitation operators were also included without selection. For the double-excitation operators, an energy threshold value was used to select the configurations on the basis of the perturbation method (vide infra). The SAC–CI was restricted to single- and double-linked operators, while the higher-order operators were treated through unlinked operators. All of the single-excitation operators were also included without selection. For the double-excitation operators in both SAC and SAC–CI, estimated using the perturbation approach, there are three levels of selection. Those which contribute with a energy threshold (in Hartree) larger than 1.0×10^{-5} (SAC) and 1.0×10^{-6} (SAC–CI) are referred to as level one, those with 5.0×10^{-6} (SAC) and 5.0×10^{-7} (SAC–CI) are level two, and those with 1.0×10^{-6} (SAC) and 1.0×10^{-7} (SAC–CI), are level three.

Finally, to be consistent with the SAC/SAC–CI ordering of the MOs where Hartree–Fock (HF) orbitals are the starting point, the molecular-orbital one-electron energies reported and used for discussion in this paper are based on the HF/6-31G level. The MO plots have been generated at this level using MOPLOT.³⁸

Results and Discussion

(a) Model Molecules. *Oxyallyl Molecule.* Trimethylene methane (TMM) is a pure biradical, and the highest-occupied orbitals are degenerate as shown in Scheme 2. The biradical character

SCHEME 2: Perturbation of the Biradical upon Substitution


of this molecule decreases upon substitution of a methylene group with a heteroatom, like oxygen, to obtain the oxyallyl molecule.^{39–40} Thus, the pure biradical with perfectly degenerate highest-occupied orbitals, from this perturbation, transforms to a biradicaloid having nearly degenerate molecular orbitals as shown in the same scheme. There is a tendency for the electron in the HOMO of the biradicaloid to occupy the LUMO because of its near degeneracy. To describe any electron transition or absorption in this biradicaloid derivative, the lowest-unoccupied orbital, which is a nonbonding orbital, has to be included into the active CI space.² Further symmetric substitution at the other two carbon atoms and geometric changes, such as variation of the angle, can also perturb the HLG, which may reflect in the electronic transitions at the CI level. As the oxyallyl molecule is the main substructure in the SQ and CR dyes, studying the transitions in this simple molecule and changing both the geometry and substitutions will help us to understand the transitions in the dyes. Keeping this in mind, we first carried out the geometry optimization of the singlet state of this model molecule at B3LYP/6-31G(d,p), and the geometry thus obtained is shown in Figure 1. This molecule will be referred as molecule **A**. The C2–O1 has a value, 1.238 Å, indicative of a resonance between a CO double bond and single bond, and the C2–C3/C2–C4 bond length, which has a value of 1.442 Å, is also between the typical double bond length and single bond length. The C3–C2–C4 angle is around 107.1°, which is reduced from the ideal sp² bond angle of 120.0°. The one-electron MOs obtained are shown in Figure 2. As expected from the symmetry, the LUMO is a nonbonding orbital with the electron density distributed on side carbons C3 and C4, while the HOMO has electron density concentrated on the oxygen atom and again on the two side carbon atoms, C3 and C4. Thus, in the LUMO, the C2 atom has no contribution due to the nodal plane, while in the HOMO, there is a very small contribution. In HOMO–2, which is a fully symmetrical orbital, the electron density is concentrated on the C–O bond, and in the LUMO+2, with three nodes the charge localization on C2 is very large. The HLG is around 7.5 eV.

Effect of Basis Set and Effect of CI Space. Two main factors affecting the SAC/SAC–CI results are the number of configurations selected into the SAC/SAC–CI space and the quality of the basis set. To understand the effect of the basis set, the SAC/SAC–CI calculations are carried out for **A** using two basis sets,

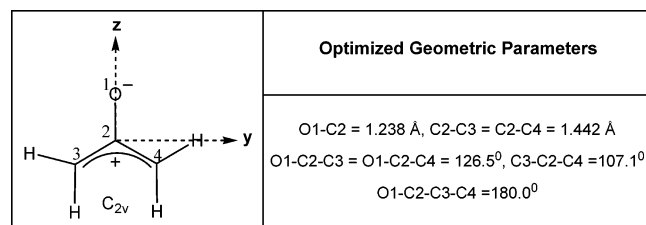


Figure 1. Geometry of the oxyallyl molecule optimized at the B3LYP/6-31G(d,p) level. The atom numbering and the coordinate system shown here is followed throughout the work.

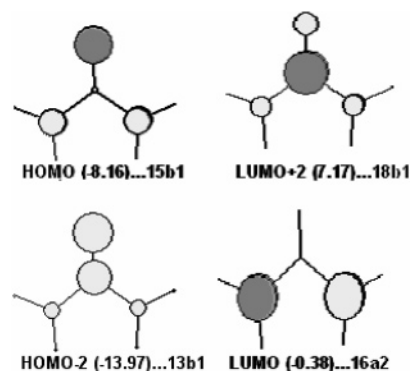


Figure 2. The one-electron molecular orbital pictures and the corresponding orbital symmetries and numbers of oxyallyl molecule obtained at the HF/6-31G level (orbital energies in eV are given in parentheses).

TABLE 1: Excitation Energy (ΔE in eV), Oscillator Strength (f), Ground-State Dipole Moment (μ_g in D), Excited-State Dipole Moment (μ_e in D) and Ground- to Excited-State Transition Dipole Moment (μ_{ge} in D) for the Oxyallyl Molecule Calculated Using the SAC/SAC–CI Method at Various Levels and Basis Sets (6-31G and 6-31G(d,p))^a with B3LYP/6-31G(d,p) Optimized Geometries^b

SAC–CI level	ΔE	f	μ_g^c	μ_e^c	μ_{ge}^d
1	2.07	0.06	–5.11	–1.61	2.76
	(1.97)	(0.06)	(–5.05)	(–1.20)	(2.92)
2	2.07	0.06	–5.13	–1.61	2.78
	(1.98)	(0.07)	(–5.10)	(–1.19)	(2.96)
3	2.10	0.06	–5.14	–1.59	2.79
	(2.05)	(0.07)	(–5.14)	(–1.18)	(2.99)

^a Values obtained with 6-31G(d,p) are given in parentheses. ^b The HOMO–LUMO gap obtained using 6-31G basis set is 7.52 eV and with 6-31G(d,p) is 7.78 eV. ^c Ground and excited dipoles are aligned along z axis (i.e., along the O1–C2 bond). ^d Transition dipole moment is aligned along the y axis.

namely, 6-31G and, with the addition of the polarization functions, 6-31G(d,p). To test the effect of the number of selected configurations on the SAC/SAC–CI results, we carried out the calculations for the same molecule at the three different levels of selection, mentioned in the earlier section under computational methods, for both the basis sets. The results are shown in Table 1. The excitation energy hardly changes in the first two levels, while there is a small change of 0.03 eV in the case of level three using the 6-31G basis set. The oscillator strength, f , hardly changes, and therefore, the transition dipole moment in changing the selection criteria also hardly changes. The ground-state dipole moment is almost constant, with only a slight change in the excited state. Thus the effect of increasing the number of configurations is small, or in other words, convergence is achieved even with a smaller number of configurations. The change in the basis set also reveals only a small change in the results. The HLG obtained is only 0.2 eV different from the increased the size of the basis set, and at the SAC/SAC–CI level, the change in the excitation energy decreases only up to 0.09 eV at level two. Keeping in mind the memory limitations because of the large size of the molecules to be studied and the very small differences in the quantitative results, we have carried out all of our SAC/SAC–CI calculations in 6-31G basis set and at level two for the B3LYP/6-31G(d,p)-optimized geometries. Thus our discussions will be based at this level.

Effect of C3–C2–C4 Angle Variation on Absorption. To understand the effect of the central angle on the absorption, we carried out the SAC/SAC–CI studies of the molecule **A** by varying the C3–C2–C4 angle from 90.0° to 125.0° in equal

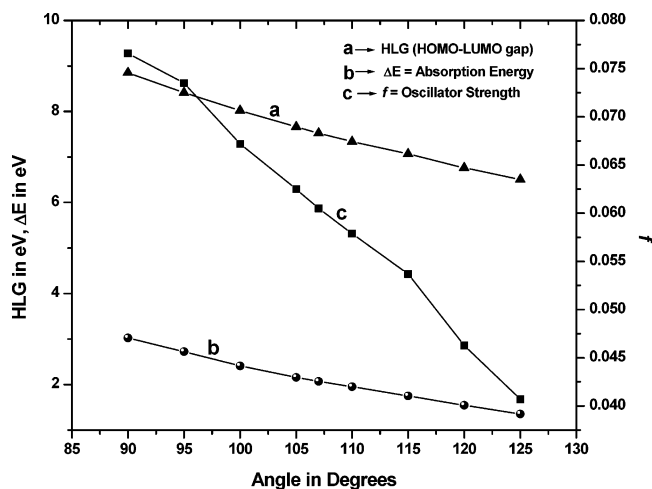
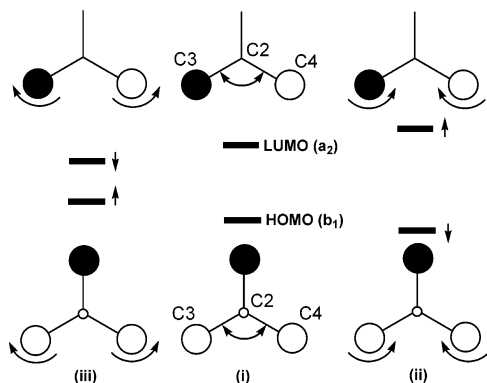


Figure 3. Effect of varying the C3–C2–C4 angle from 90° to 125° on HLG, absorption energy, and oscillator strength for the oxyallyl molecule (values obtained from SAC/SAC–CI calculations). The optimized point at 107.1° is also shown.

SCHEME 3: Effect of Varying the C3–C2–C4 Bond Angle on (i) HOMO and LUMO Molecular Orbital Energy Levels (orbital symmetry symbols are given in parentheses). Decrease and Increase in the Bond Angles Are Shown in (ii) and (iii), Respectively



intervals, but we did no further geometry optimization. The variation of the HLG, ΔE , and f with respect to the change in angle is shown in Figure 3. It is very interesting to note that as the angle increases the HLG decreases. Thus, the HLG, which is 8.85 eV at an angle of 90.0°, decreased by 2.34 eV at an angle of 125.0°. At the SAC/SAC–CI level, the ΔE behaves in a similar fashion. At an angle of 125.0°, the absorption is 1.36 eV which corresponds to a nearly 900 nm absorption wavelength. The oscillator strength on the other hand decreases when the angle is increased and is weak in the long-wavelength region. From the graph (Figure 3), it can be seen that the HLG variation and ΔE follow a similar trend; in other words, the HLG alone is sufficient to understand the absorption of the molecule. The observation that an absorption of nearly 1000 nm can be achieved just by varying the angle is very interesting; in fact for the BM dye, Tatsuura et al.⁶ reported an absorption of around 1100 nm for which the central angle obtained from the X-ray analysis⁵ was 124.5°. The changes in HLG or ΔE can be easily explained by observing the variation of the one-electron MOs with respect to angle in Scheme 3.

In the HOMO, as the angle becomes smaller, the bonding combination of C3 and C4 orbitals increases. This stabilizes the HOMO, or in other words, the energy decreases. In the LUMO, as the angle becomes smaller, the antibonding combination of C3 and C4 destabilizes the orbital and the energy

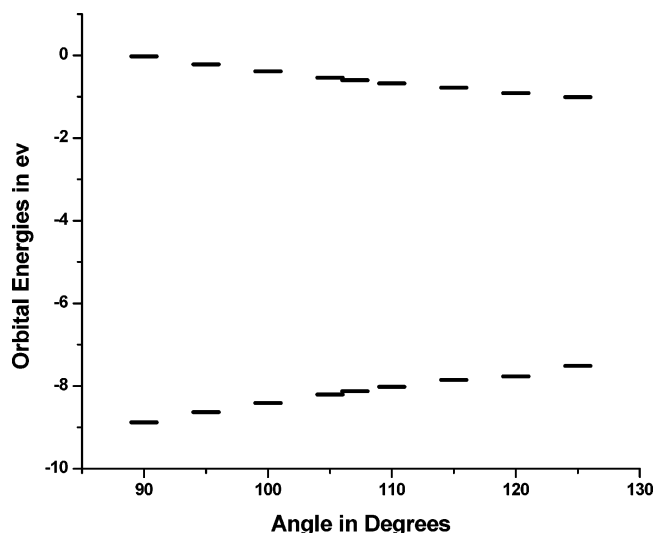


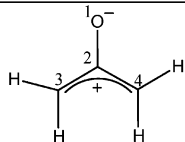
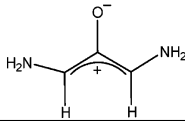
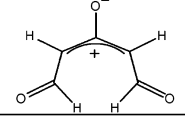
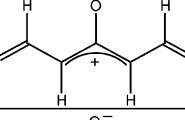
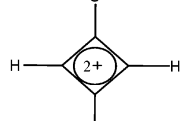
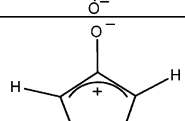
Figure 4. Effect of varying the C3–C2–C4 angle from 90° to 125° on the HOMO–LUMO energies of the oxyallyl molecule.

increases. Thus the net result is that when the angle decreases, the HLG increases and vice versa when the angle increases. This is clearly shown in Figure 4 in which the one-electron energies of the HOMO and LUMO are plotted against the changing angles.

Effect of Substitution on Absorption. In the earlier section, we have shown that geometry plays a major role in absorption, and even without any substitutions, the absorption can be shifted to 1000 nm. Here, we study the effect of substituting groups on the oxyallyl molecule. We have chosen five molecules which are shown in Table 2. We have also included the unsubstituted oxyallyl molecule, **A**, for comparison. To understand the effect of substituting electron-donating groups, such as the amino, we have chosen molecule **B**, and for the effect of substituting electron-withdrawing groups, such as the carbonyl, we have included **C** and **D**. Molecules **C** and **D** differ in conformation, but the withdrawing groups remain the same; the difference will be discussed in detail later. We have also carried out the SAC–CI calculations on the simple SQ and CR dyes, and these are shown as **E** and **F**, respectively, in the table. The optimization of all of these molecules in the lowest-singlet states was carried out at the B3LYP/6-31G(d,p) level for the respective symmetries as shown in the table. The details of the geometrical parameters thus obtained are shown in the same table. Molecule **A**, the simple oxyallyl molecule, has a C2–O1 bond length of 1.238 Å, which does not change upon substituting with electron-withdrawing groups, as in **C** and **D**. But this bond length elongates to 1.282 Å and has a more single-bond character in the molecule substituted with amino groups, **B**. In the simple SQ and CR molecules, there is a shortening of this bond, indicating a larger resonance contribution. In the case of the C2–C3 bond, molecule **B** has a larger double bond character, and this bond is shortened by 0.03 Å compared to that of **A**, while in all other cases, there is an increase in the bond length, with the simple SQ molecule having a lengthening of as much as 0.04 Å. In general, the variation of the bond length indicates that, in the case of **B**, there is a more zwitterionic character and less resonance. Bond angle C3–C2–C4 is 107.1° in the unsubstituted **A** and increases in **B**. In **C** and **D**, because of the conformational difference, there is a change of 11° with **C** having the larger angle of 120.2°.

The excitation energies along with oscillator strength and dipole moments of the model molecules are shown in Table 3. In the unsubstituted molecule, the SAC–CI calculations reveal

TABLE 2: Optimized Geometrical Parameters of All Model Molecules Calculated at the B3LYP/6-31G(d,p) Level^a

Molecule	Structure	Sym	Bond Lengths (Å)		Bond Angles (deg)	
			O1-C2	C2-C3	O1-C2-C3	C4-C2-C3
A		C _{2v}	1.238	1.442	126.5	107.1
B		C _{2v}	1.282	1.411	122.5	115.1
C		C _{2v}	1.236	1.462	119.9	120.2
D		C _{2v}	1.238	1.453	125.2	109.7
E		D _{2h}	1.212	1.481	136.8	86.4
F		C _{2v}	1.223	1.466	128.6	102.8

^a The numbering of atoms depicted in molecule **A** is the same for all other molecules in this work.

TABLE 3: HOMO–LUMO Gap (HLG in eV), Excitation Energy (ΔE in eV), Oscillator Strength (f), Ground-State Dipole Moment (μ_g in D), Excited-State Dipole Moment (μ_e in D) and Ground- to Excited-State Transition Dipole Moment (μ_{ge} in D) for Model Molecules A–F, Calculated Using the SAC/SAC–CI Method (level two/6-31G) for the Optimized Geometries of the Respective Molecules

molecule	HLG	ΔE	f	transition	μ_g^a	μ_e^a	μ_{ge}^b
A	7.52	2.07	0.06	¹ A ₁ – ¹ B ₂	–5.13	–1.61	2.78
B	8.53	3.09	0.37	¹ A ₁ – ¹ B ₂	–4.74	–2.14	5.64
C	5.70	1.25	0.10	¹ A ₁ – ¹ B ₂	–2.56	1.32	4.53
D	6.35	1.53	0.13	¹ A ₁ – ¹ B ₂	–2.12	1.41	4.69
E	8.73	2.89	0.07	¹ A _g – ¹ B _{2u}	0.00	0.00	2.49
F	6.87	1.99	0.10	¹ A ₁ – ¹ B ₂	0.94	4.09	3.66

^a μ_g and μ_e are aligned along the z axis. ^b μ_{ge} is aligned along the y axis.

a excitation energy of only 2.07 eV between the ground and excited states despite the large HLG of 7.5 eV. This corresponds to an absorption of around 600 nm in wavelength. The oscillator strength is weak and is only 0.06. The dipole moment is in the direction of z axis, passes through the carbonyl group, C2–O1, and has a change of around 4.0 D when excited. The magnitude decreases in the excited state. The transition dipole moment is not very large and has a magnitude of 2.78 D along the y axis, which is the long axis. Molecule **B** has a very large HLG, and its absorption energy at the CI level is 3.09 eV. This indicates that upon substituting a simple oxyallyl molecule with electron donating groups, the HLG and the absorption increase, but the oscillator strength is quite large and has a value of 0.37. The dipole moment change upon excitation is not very large,

but the transition dipole moment is large. On the other hand, in **C** and **D**, the HLG is much smaller, and this is also reflected in the excitation energy. The ΔE in **C** is only 1.25 eV, which in terms of wavelength is around 1000 nm. The oscillator strength is much smaller. In **D**, which has a smaller C3–C2–C4 angle of 109.7°, the HLG increases and the absorption is now 1.53 eV. This again indicates the importance of the C3–C2–C4 angle in the variation of the absorption even though the substitution remains the same. In the simple SQ and CR molecules, the HLG is larger in SQ, and this is again reflected in the ΔE of 2.89 eV, when compared to 1.99 eV in the simple CR. One notable point is that in all of the molecules the dipole moment increase in the excited state is between 3 and 4.0 D, while in the case of the simple SQ it does not change at all because of the symmetry.

The details of the SAC–CI of all the model molecules are shown in Table 4. The ground-state symmetry and the excited-state symmetry along with the dominant configurations are shown. The number of main configurations which have a contribution of more than 0.03 is given in the fifth column. In the last column, the number of linked operators generated and selected are indicated. To understand the transitions, we use the one-electron MOs of **A** shown in Figure 2. The ground state configuration is dominated by the HF configuration. Small contributions from the double-excited configurations, namely, double excitation into the LUMO, is seen. In this excitation, the electron density distributes from the central part of the molecule to the sides. The excitation from HOMO–2 to LUMO and HOMO–LUMO is also of a similar nature. The major

TABLE 4: Main Configurations, Mixing Coefficients, Number of Configurations and Linked Operators for the Singlet Ground State and Excited State Obtained from the SAC/SAC–CI Calculation at the B3LYP/6-31G(d,p) Optimized Geometries of Model Molecules

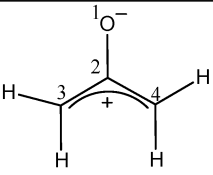
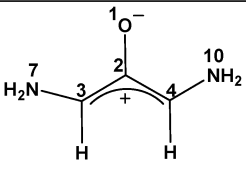
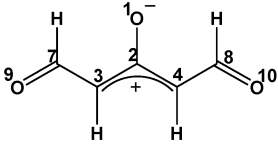
molecule	state	mixing coefficient ^{a,d}	configuration ^e	no. of configurations ^b	linked operators ^c
A	¹ A ₁	1.000	15b ₁ ² , 16a ₂ ⁰	18	14791/6398
		0.075	15b ₁ –18b ₁		
		–0.221	15b ₁ –16a ₂ , 15b ₁ –16a ₂		
		0.202	15b ₁ –16a ₂ , 13b ₁ –16a ₂		
		–0.055	13b ₁ –18b ₁ , 13b ₁ –18b ₁		
	¹ B ₂	0.847	15b ₁ –16a ₂	18	14568/3266
		0.378	13b ₁ –16a ₂		
		–0.377	15b ₁ –18b ₁ , 15b ₁ –16a ₂		
		–0.122	15b ₁ –18b ₁ , 13b ₁ –16a ₂		
		–0.081	15b ₁ –40b ₁ , 15b ₁ –16a ₂		
B	¹ A ₁	1.000	23b ₁ ² –24a ₂ ⁰	11	74817/18243
		–0.098	23b ₁ –24a ₂ , 23b ₁ –24a ₂		
		0.052	23b ₁ –24a ₂ , 18b ₁ –24a ₂		
	¹ B ₂	0.913	23b ₁ –24a ₂	14	74388/8880
		0.208	21b ₁ –24a ₂		
		0.113	18b ₁ –24a ₂		
		–0.305	23b ₁ –29b ₁ , 23b ₁ –24a ₂		
		–0.084	23b ₁ –29b ₁ , 21b ₁ –24a ₂		
		–0.084	20a ₂ –24a ₂ , 18b ₁ –24a ₂		
C	¹ A ₁	1.000	29b ₁ ² –30a ₂ ⁰	32	159703/25808
		–0.153	29b ₁ –30a ₂ , 29b ₁ –30a ₂		
		0.096	29b ₁ –30a ₂ , 25b ₁ –30a ₂		
		–0.069	29b ₁ –32a ₂ , 21b ₁ –30a ₂		
		0.068	29b ₁ –30a ₂ , 21b ₁ –30a ₂		
		–0.061	24a ₂ –32a ₂ , 21b ₁ –31b ₁		
		–0.058	29b ₁ –31b ₁ , 24a ₂ –30a ₂		
		–0.055	24a ₂ –31b ₁ , 21b ₁ –32a ₂		
		–0.054	24a ₂ –32a ₂ , 24a ₂ –30a ₂		
		0.052	29b ₁ –32a ₂ , 29b ₁ –30a ₂		
	¹ B ₂	0.840	29b ₁ –30a ₂	23	159104/13610
		0.358	25b ₁ –30a ₂		
		0.138	21b ₁ –30a ₂		
		0.272	29b ₁ –31b ₁ , 29b ₁ –30a ₂		
		–0.253	29b ₁ –35b ₁ , 29b ₁ –30a ₂		
D	¹ A ₁	1.000	29b ₁ ² –30a ₂ ⁰	28	159703/25650
		–0.134	29b ₁ –30a ₂ , 29b ₁ –30a ₂		
		0.078	29b ₁ –30a ₂ , 22b ₁ –30a ₂		
		0.074	29b ₁ –30a ₂ , 25b ₁ –30a ₂		
		–0.063	29b ₁ –32a ₂ , 22b ₁ –30a ₂		
		0.059	29b ₁ –32a ₂ , 29b ₁ –30a ₂		
		0.057	25b ₁ –31b ₁ , 24a ₂ –30a ₂		
		0.055	25b ₁ –32a ₂ , 24a ₂ –31b ₁		
		–0.054	24a ₂ –32a ₂ , 24a ₂ –30a ₂		
		0.053	25b ₁ –31b ₁ , 24a ₂ –32a ₂		
	–0.052	24a ₂ –32a ₂ , 22b ₁ –31b ₁			
	¹ B ₂	0.847	29b ₁ –30a ₂	22	159104/13706
		0.335	25b ₁ –30a ₂		
		0.179	22b ₁ –30a ₂		
		–0.250	29b ₁ –34b ₁ , 29b ₁ –30a ₂		
0.250		29b ₁ –31b ₁ , 29b ₁ –30a ₂			
E	¹ A _g	1.000	21b _{3u} ² –22b _{1g} ⁰	28	21693/9065
		0.143	21b _{3u} –22b _{1g} , 16b _{3u} –22b _{1g}		
		–0.127	21b _{3u} –22b _{1g} , 21b _{3u} –22b _{1g}		
		–0.068	18b _{2g} –27b _{3u} , 16b _{3u} –23b _{2g}		
		–0.065	18b _{2g} –23b _{2g} , 16b _{3u} –27b _{3u}		
		–0.065	21b _{3u} –23b _{2g} , 21b _{3u} –23b _{2g}		
		–0.059	21b _{3u} –27b _{3u} , 18b _{2g} –23b _{2g}		
		–0.057	18b _{2g} –23b _{2g} , 18b _{2g} –23b _{2g}		
		0.054	21b _{3u} –23b _{2g} , 20b _{3g} –29b _{2u}		
		¹ B _{2u}	0.898		
	0.245		16b _{3u} –22b _{1g}		
	0.074		20b _{3g} –26b _{1u}		
	–0.262		21b _{3u} –27b _{3u} , 21b _{3u} –22b _{1g}		
	–0.231		21b _{3u} –23b _{2g} , 18b _{2g} –22b _{1g}		
		–0.130	21b _{3u} –22b _{1g} , 18b _{2g} –23b _{2g}		

TABLE 4: (Continued)

molecule	state	mixing coefficient ^{a,d}	configuration ^e	no. of configurations ^b	linked operators ^c
F	¹ A ₁	1.000	28b ₁ ² -29a ₂ ⁰	25	126396/25006
		-0.128	28b ₁ -29a ₂ , 28b ₁ -29a ₂		
		0.078	28b ₁ -29a ₂ , 23b ₁ -29a ₂		
		0.074	28b ₁ -29a ₂ , 21b ₁ -29a ₂		
		0.070	25a ₂ -34a ₂ , 21b ₁ -30b ₁		
		0.068	28b ₁ -30b ₁ , 25a ₂ -29a ₂		
		0.057	25a ₂ -30b ₁ , 21b ₁ -34a ₂		
		-0.053	25a ₂ -34a ₂ , 25a ₂ -29a ₂		
	¹ B ₂	0.050	28b ₁ -29a ₂ , 25a ₂ -30b ₁	20	125844/11952
		0.871	28b ₁ -29a ₂		
		0.302	23b ₁ -29a ₂		
		0.129	21b ₁ -29a ₂		
		-0.284	28b ₁ -32b ₁ , 28b ₁ -29a ₂		
		0.152	28b ₁ -30b ₁ , 23b ₁ -29a ₂		
		0.146	28b ₁ -30b ₁ , 28b ₁ -29a ₂		
		-0.125	28b ₁ -32b ₁ , 23b ₁ -29a ₂		
-0.073	28b ₁ -29a ₂ , 23b ₁ -32b ₁				

^a CI coefficients for the ground state are larger than 0.05, and for the excited state, they are larger than 0.07. ^b Number of configurations that have a CI coefficient larger than 0.03. ^c Linked operators total generated/selected. ^d For the SAC, by definition, the coefficient of HF configuration is always 1.00. ^e Orbital numbers and orbital symmetries along with occupation.

TABLE 5: Stabilization Energy (*E* in kcal/mol) Associated with Delocalization of the Interactions, Which Give Strongest Stabilization Obtained from NBO Analysis^a

Molecule	Donor	Occupation	Acceptor	Occupation	E
	BD (1) O 1- C 2	1.997	LP (1) C 3	0.748	11.16
	BD (1) O 1- C 2	1.997	LP*(1) C 4	0.748	11.16
	LP (1) O 1	1.976	RY*(1) C 2	0.017	15.63
	LP (2) O 1	1.862	BD*(1) C 2- C 3	0.066	22.00
	LP (2) O 1	1.862	BD*(1) C 2- C 4	0.066	22.00
	LP (1) C 3	0.748	BD*(1) O 1- C 2	0.496	54.29
	LP*(1) C 4	0.748	BD*(1) O 1- C 2	0.496	54.29
		LP (1) O 1	1.976	RY*(1) C 2	0.014
LP (2) O 1		1.852	BD*(1) C 2- C 3	0.054	15.83
LP (2) O 1		1.852	BD*(1) C 2- C 4	0.054	15.83
LP (3) O 1		1.705	LP (1) C 2	1.021	187.43
LP (1) C 2		1.021	BD*(2) C 3- N 7	0.634	310.43
LP (1) C 2		1.021	BD*(2) C 4- N10	0.634	310.43
	BD (2) O 1- C 2	1.990	LP (1) C 3	0.765	10.46
	BD (2) O 1- C 2	1.990	LP*(1) C 4	0.765	10.46
	BD (2) C 7- O 9	1.914	LP (1) C 3	0.765	15.46
	BD (2) C 8- O10	1.914	LP*(1) C 4	0.765	15.46
	LP (1) O 1	1.977	RY*(1) C 2	0.017	15.11
	LP (2) O 1	1.868	BD*(1) C 2- C 3	0.065	21.10
	LP (2) O 1	1.868	BD*(1) C 2- C 4	0.065	21.10
	LP (1) C 3	0.765	BD*(2) O 1- C 2	0.433	56.28
	LP (1) C 3	0.765	BD*(2) C 7- O 9	0.103	33.71
	LP*(1) C 4	0.765	BD*(2) O 1- C 2	0.433	56.28
	LP*(1) C 4	0.765	BD*(2) C 8- O10	0.103	33.71
	LP (2) O 9	1.904	BD*(1) C 3- C 7	0.047	18.25
	LP (2) O 9	1.904	BD*(1) C 7- H11	0.054	18.21
	LP (2) O10	1.904	BD*(1) C 4- C 8	0.047	18.25
LP (2) O10	1.904	BD*(1) C 8- H12	0.054	18.21	

^a BD and BD* correspond to bonding and antibonding orbitals, respectively. LP and LP* correspond to bonding and antibonding lone pairs, respectively. RY* correspond to antibonding Rydberg-type of orbitals. In the parentheses, 1 represents σ and 2 and 3 represent π -type orbitals.

transitions of all model molecules are nearly same. It is the transition between the perturbed biradical orbitals which are now the HOMO and the LUMO. What was a perfectly zero transition in the biradical state is now shifted to a very long-wavelength region with a weak oscillator strength (small ΔE). In the case of **B**, there is a slightly smaller contribution of the double excitation compared to that of **C** and **D**. The one-electron MOs

of all other molecules are given in the Supporting Information (Figure 1).

Thus, it is clear that the HLG plays the crucial role in the absorption, and the effect of the substitution is to perturb this gap. A substitution with a group like the amino results in an increase of the HLG, even though the C3-C2-C4 angle is around 115°. To understand the perturbation, we carried out an

TABLE 6: Charge Transfer from Ground to Excited States of All Model Molecules

molecule	group	ground	excited	gain/loss ^a
A	I	-0.59	-0.24	-0.35
	II	0.59	0.24	0.35
B	I	-0.75	-0.46	-0.29
	II	0.91	0.72	0.19
	III	-0.16	-0.25	0.09
C	I	-0.58	-0.24	-0.34
	II	0.53	0.25	0.28
	III	0.05	-0.01	0.06
D	I	-0.61	-0.25	-0.36
	II	0.49	0.27	0.22
	III	0.12	-0.02	0.14
E	I	-0.92	-0.63	-0.29
	II	0.92	0.63	0.29
F	I	-1.33	-1.11	-0.22
	II	1.33	1.11	0.22

^a Represents the gain/loss of electron charge density (in e) in the respective groups upon excitation of the molecule from the ground to excited state. Loss is shown as negative sign.

NBO analysis of the molecules **A** (unsubstituted oxallyl), **B** (amino groups substituted), and **D** (carbonyl groups substituted). We have chosen only these three molecules because they should be able to give a complete picture of the perturbation. The simple NBO analysis for three model molecules was carried out using the ab initio software G03W.³⁷ In an ideal Lewis-type bond, the valence antibonds are unoccupied, but because of delocalization, electrons occupy these antibonding orbitals and a deviation occurs. The energetic stabilization from such interactions (i.e., the donor-acceptor interactions between the occupied orbitals and the antibonding orbitals) are estimated using a second-order perturbation theory.^{41a,b} These are shown in Table 5. The large perturbations in **A** and **D** are basically the result of side carbons C3 and C4 being perturbed by the C2–O1 bond. Thus, the perturbation is as much as 54–56 kcal/mol in these molecules. On the other hand, there is a very large perturbation in **B** from the C3–N7 and C4–N10 bonds interacting with the p orbital of C2. This perturbation causes the HLG to increase.

Charge Transfer in the Model Molecules. The next question we propose to answer is does the geometry or substitution influence the charge transfer. We have compiled the charge-transfer data in Table 6. These are the Mulliken charges obtained both at the SAC and SAC–CI levels. The molecule is divided into three parts for understanding the charge flow. The first part is the oxygen atom(s), group I, the second one is the main ring, group II, and finally the third, which are the substituted groups, group III. In the simple oxallyl molecule, **A**, the charge on the oxygen atom at the SAC level is 0.59 e, and it decreases in the excited state to 0.24 e, with a net flow of 0.35 e to the ring. Upon substitution with amino groups, molecule **B**, the charge transfer from the oxygen atom to the ring decreases slightly and is now 0.29 e. The amino groups gain about 0.09 e in the excited state. When substituted by withdrawing groups such as the carbonyl in molecules **C** and **D**, the net charge transfer from the oxygen atom does not change much and remains nearly same

as in **A**, but there is a small increase in the gain of charge in the side carbonyl groups in the excited state of **D**. Individually, the oxygen atoms (there are two of them) in **E** have smaller charge localizations of 0.92 e in the ground state when compared to those of **F** at 1.33 e, where there are three oxygen atoms, but the amount of charge transferred from group I to II hardly has any change in both these molecules, and they remain around 0.29–0.22 e. On the basis of the absorption data obtained earlier, **F** has a very small excitation energy when compared to that of **E**. This leads us to infer that charge transfer may not play the key role in the red shift in **F**. Further proof is obtained in the variation of the oxallyl C3–C2–C4 angle, where the ΔE is red shifted with the increasing angle, but the charge transfer remains nearly the same (Supporting Information, Table A).

(b) SQ and CR Derivatives. We have chosen nine molecules of which five are SQ derivatives and another four are CR derivatives. These are shown in Table 7. Molecule **1** and **6** are simplest SQ dye and CR dye with electron-donating group –NH₂ substituted at the C3 and C4 position. The effect of increasing the conjugation, by substituting an aniline moiety, is seen in molecules **2**, **3**, and **7**. Molecule **3** is included in the SQ derivative to understand the effect of the –OH groups. Molecules **4** and **8** are the derivatives of chalcogenopyrylium with oxygen as the heteroatom in the ring. To understand the effect of replacing this oxygen atom with larger atom like sulfur, we also include molecules **5** and **9**. It should be noted that for molecules **4**, **5**, **8**, and **9** there are other symmetries, namely, the C_{2h}/C_s groups, which also turn out to be minima. In the relative stabilities, the more symmetric point groups are slightly less stable by less than 1 kcal/mol in some cases. For the sake of clarity, we report only the energies of the highly symmetric groups as we find that there is very little difference in the transitions and other details. The details of the excitation analysis for the lower symmetries are given in the Supporting Information (Figure 2 and Table B). The experimental data, like the absorption, for all of these molecules are available in the literature; therefore, a direct comparison with results obtained by theoretical calculations is possible. The singlet–triplet (S–T) energy gap calculated at the B3LYP/6-31G(d,p) level is also shown in Table 7. These values along with the geometrical parameters for the singlets are in the same table.

The variation in the C2–O1 bond length is very small. When compared to the bond length of unsubstituted oxallyl molecule, **A**, the bond lengths vary only up to 0.01 Å. In the case of the C3–C2 bond length, the variation is up to 0.03 Å, but the C3–C2–C4 angle varies from 86° in the SQ derivatives to 112° in the CR derivatives. One interesting observation is that, in the chalcogenopyrylium dye derivatives, changing the heteroatom from oxygen to sulfur does not affect the geometry in both SQ and CR derivatives. On the other hand, direct substitution of the amino groups on the dyes (**1** and **6**) yield smaller angles when compared to increasing the conjugation (**2** and **7**).

The HLG, SAC/SAC–CI studies are shown in Table 8 for all of these molecules. The HLG values are in general smaller than the model molecules. In the case of **1** and **6**, there is a larger HLG, as expected. The smaller HLG is also reflected in the singlet–triplet gap in Table 7. Thus, the S–T gap in molecule **9** is only 6.4 kcal/mol while its HLG is only 4 eV. On the other hand, again **1** and **6**, in their respective series, have the largest S–T gaps. A smaller S–T gap suggests a larger biradical character. In general, the CR dyes have smaller HLG values than the SQ dyes. In the case of the chalcogenopyrylium dyes, the substitution of sulfur for oxygen reduces the HLG. The ΔE values follow the HLG trend clearly reproducing the

TABLE 7: Optimized Geometric Parameters for All Molecules Calculated at the B3LYP/6-31G(d,p) Level^a

Molecule	Structure	Sym	Bond Lengths (Å)		Bond Angles (deg)		$\Delta E(S-T)^c$
			O1-C2 (O6-C5)	C2-C3 (C2-C4)	O1-C2-C3 (O1-C2-C4)	C3-C2-C4 (C4-C5-C3)	
1		D _{2h}	1.227	1.469	136.5	86.9	52.2
2		C _{2h}	1.230	1.475	135.6	88.8	25.8
3		C _{2h}	1.253	1.460	133.9	92.2	33.6
4 ^b		C _{2v}	1.240	1.477	135.1	89.9	16.4
		C _{2h}	(1.223)	1.481	135.2	(89.6)	16.5
5 ^b		C _{2v}	1.238	1.478	135.0	90.0	13.0
		C _{2h}	(1.222)	1.483	135.2	89.7	13.1
6		C _{2v}	1.240	1.448	128.3	103.4	28.3
		C ₂	1.268	1.463	123.7	112.6	16.6
7		C _{2v}	1.250	1.466	126.4	107.3	8.4
		C _s	1.243	1.477	123.5	107.9	7.8
8		C _{2v}	1.249	1.467	126.3	107.5	6.4
		C _s	1.242	1.480	123.4	108.0	5.8
9		C _s	(1.465)	(128.6)			

^a The numbering system adopted for molecule 1 is followed for molecules 2–5 and numbering system adopted for molecule 6 is followed for molecules 7–9. ^b In molecules 4 and 5 (C_{2v}) the bond lengths, 1.481 Å and 1.483 Å, are the bond lengths between C4–C5 and the angle 135.2° is the angle between O6–C5–C4. ^c $\Delta E(S-T) = E_{\text{triplet}} - E_{\text{singlet}}$ is the singlet–triplet energy gap (values are in kcal/mol).

behavior in the model molecules. The excitation energies, in general, are in good agreement with the experimental values. The transition dipole moments are larger suggesting a larger polarizability, but the changes in the dipole moments are much smaller when compared to the model molecules. The charge transfer, based on the Mulliken charge densities, is shown in Table 9. There is hardly any charge transfer from one part of the molecule to the other in the molecules even with a very low-excitation energy. The largest charge transfer is seen in 1, where the excitation energy happens to actually be large. In the case of 7 and 9, the oxygens seem to act as electron acceptors in the excited state (very small charge transfer). It

should be pointed out that we have assumed that the two carbonyl oxygens act as electron donors (dominant zwitterionic structure). When we check the charges of the individual oxygen atoms, there is no substantial charge transfer (Supporting Information, Table C). Our main focus is on the donating groups, R, and except in molecule 3, where there is donation of 0.16 e to the ring, in all other molecules it is very small. Thus, there is no correlation of the low-excitation energy and charge transfer. The SAC/SAC–CI details for all molecules are shown in Table 10, and basically, like in the model molecules, these are double excitations which mix up in the ground state. The S₀–S₁ transition is dominated by the HOMO–LUMO excitation.

TABLE 8: HOMO–LUMO Gap (HLG in eV), Excitation Energy (ΔE in eV), Oscillator Strength (f), Experimental Excitation Energy (in eV), Ground-State Dipole Moment (μ_g in D), Excited-State Dipole Moment (μ_e in D) and Ground- to Excited-State Transition Dipole Moment (μ_{ge} in D) for All Molecules 1–9, Calculated Using the SAC/SAC–CI (level two/6-31G) Method for Optimized Geometries

molecule	symmetry	HLG	ΔE	$\times c4$	exptl ΔE	transition	μ_g	μ_e	μ_{ge}	
									X	Y
1	D_{2h}	9.73	4.30	0.47	4.34 ^a	$^1A_g-^1B_{2u}$	0.00	0.00	0.00	5.36
2	C_{2h}	6.67	2.22	1.25	1.98 ^b	$^1A_g-^1B_u$	0.00	0.00	0.02	12.18
3	C_{2h}	6.87	2.02	1.17	1.89 ^c	$^1A_g-^1B_u$	0.00	0.00	0.02	12.37
4	C_{2v}	5.75	1.76	1.18	1.74 ^d	$^1A_1-^1B_2$	-3.37	-3.06	0.00	13.32
5	C_{2v}	5.24	1.54	1.31	1.54 ^d	$^1A_1-^1B_2$	-3.16	-3.27	0.00	14.97
6	C_{2v}	7.73	3.13	0.47	2.82 ^e	$^1A_1-^1B_2$	3.03	4.32	0.00	-6.29
7	C_2	5.50	1.52	1.13	1.44 ^f	$^1A-^1B$	4.47	5.41	-0.25	-14.00
8	C_{2v}	4.76	1.48	1.10	1.47 ^g	$^1A_1-^1B_2$	7.52	7.66	0.00	14.00
9	C_{2v}	4.30	1.27	1.20	1.31 ^g	$^1A_1-^1B_2$	7.41	7.99	0.00	15.78

^a Ref 43. ^b Ref 13. ^c Ref 12. ^d Ref 42. ^e Ref 2. ^f Ref 6. ^g Ref 22.

TABLE 9: Charge Transfer from Ground to Excited States of All SQ and CR Molecules

Group I: O⁻

Group II: O⁻

Group III: R

Group I: O⁻

Group II: O⁻

Group III: R

molecule	group	ground	excited	gain/loss ^a
1	I	-1.05	-0.83	-0.22
	II	1.24	1.07	0.17
	III	-0.20	-0.24	0.04
2	I	-1.16	-1.07	-0.09
	II	0.52	0.34	0.18
	III	0.64	0.73	-0.09
3	I	-1.44	-1.40	-0.04
	II	0.55	0.37	0.18
	III	0.88	1.04	-0.16
4	I	-1.19	-1.13	-0.06
	II	0.54	0.43	0.11
	III	0.65	0.70	-0.05
5	I	-1.18	-1.14	-0.04
	II	0.54	0.44	0.10
	III	0.64	0.70	-0.06
6	I	-1.54	-1.38	-0.16
	II	1.69	1.59	0.10
	III	-0.15	-0.20	0.05
7	I	-1.96	-2.01	0.05
	II	1.13	1.12	0.01
	III	0.83	0.90	-0.07
8	I	-1.69	-1.68	-0.01
	II	1.01	0.96	0.05
	III	0.67	0.72	-0.05
9	I	-1.67	-1.70	0.03
	II	1.00	0.97	0.03
	III	0.67	0.73	-0.06

^a Represents the gain/loss of electron charge density (in e) in the respective groups upon excitation of the molecule from the ground to excited state. Loss is shown as negative sign. There is rounding error of up to 0.02 e in some cases.

(C) SQ Derivatives with Extended Conjugation. We now turn our attention to the experiment conducted by Meier et al., where increasing the conjugation showed a red shift followed by blue shift for a further increase of the conjugation.¹² A systematic SAC/SAC–CI study by increasing the number of conjugated units to the SQ ring shown in Figure 5 is beyond

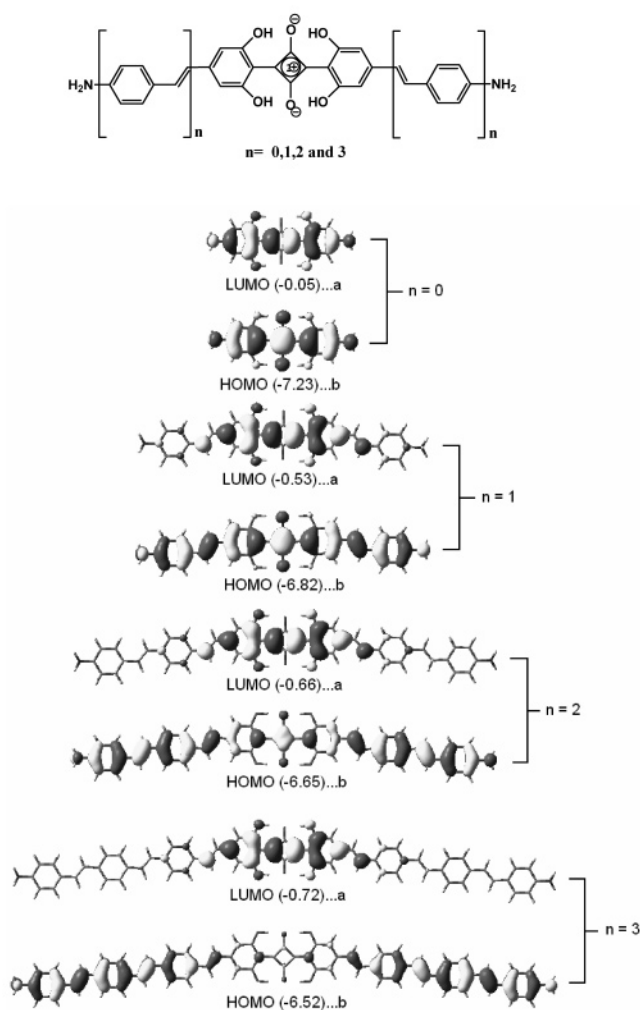


Figure 5. Frontier molecular orbital pictures of stilbinoid SQ derivatives obtained from GaussView.³⁷ All the orbitals shown here are with default iso value of 0.02.

the scope of this paper. But we should be able to explain the observation, at least qualitatively, on the basis of the one-electron MOs shown in the same figure whose geometries are obtained at the B3LYP/6-31G(d,p) level. From $n = 0$ to 1 there is not much difference in the central part of the molecule, indicating that the MOs of oxyallyl characteristics are retained in the HOMO and LUMO. But upon increasing the conjugation, there is drop in the charge density in the HOMO at the central part of the molecule, and in the case of $n = 3$, the oxyallyl substructure does not contribute to the HOMO. Although the

TABLE 10: Main Configurations, Mixing Coefficients, Number of Configurations, and Linked Operators for the Singlet Ground State and Excited States Obtained from the SAC/SAC–CI Calculation at B3LYP/6-31G(d,p) Optimized Geometries

molecule	state	mixing coefficient ^{a,d}	configuration ^e	no. of configurations ^b	linked operators ^c
1	¹ A _g	1.000	29b _{3u} ² , 30b _{1g} ⁰	18	79151/19193
		-0.071	29b _{3u} -30b _{1g} , 29b _{3u} -30b _{1g}		
	-0.060	29b _{3u} -31b _{2g} , 29b _{3u} -31b _{2g}	17	78224/8745	
	0.051	29b _{3u} -30b _{1g} , 22b _{3u} -30b _{1g}			
	-0.050	25b _{2g} -31b _{2g} , 25b _{2g} -31b _{2g}			
	¹ B _{2u}	-0.937			29b _{3u} -30b _{1g}
		0.106			22b _{3u} -30b _{1g}
	-0.096	26b _{3u} -30b _{1g}			
	-0.069	28b _{3g} -34b _{1u}			
	-0.205	29b _{3u} -36b _{3u} , 29b _{3u} -30b _{1g}			
	-0.156	29b _{3u} -31b _{2g} , 25b _{2g} -30b _{1g}			
	-0.081	29b _{3u} -30b _{1g} , 25b _{2g} -31b _{2g}			
	-0.081	26b _{3u} -30b _{1g} , 24b _{1g} -30b _{1g}			
2	¹ A _g	1.000	69b _u ² , 70a _g ⁰	6	10872349/65032
	-0.050	67b _g -71b _g , 66a _u -73a _u	16	10867688/62083	
¹ B _u	0.952	69b _u -70a _g			
	-0.084	68a _g -72b _u			
0.078	52b _u -70a _g				
0.106	69b _u -72b _u , 69b _u -70a _g				
0.095	69b _u -70a _g , 68a _g -70a _g				
0.075	69b _u -75a _g , 68a _g -70a _g				
-0.075	68a _g -70a _g , 65b _u -70a _g				
-0.075	69b _u -74b _g , 59b _g -70a _g				
3	¹ A _g	1.000	85b _u ² , 86a _g ⁰	3	11187127/73975
	¹ B _u	0.948	85b _u -86a _g	18	11182400/65786
-0.085	82a _g -88b _u				
0.147	85b _u -86a _g , 82a _g -86a _g				
0.099	85b _u -86a _g , 79a _g -86a _g				
0.092	85b _u -88b _u , 85b _u -86a _g				
0.083	85b _u -91a _g , 79a _g -86a _g				
0.079	85b _u -91a _g , 82a _g -86a _g				
0.079	85b _u -91a _g , 82a _g -86a _g				
4	¹ A ₁	1.000	69b ₁ ² , 70a ₂ ⁰	12	3203419/49360
		0.057	65b ₁ -73b ₁ , 64a ₂ -72a ₂		
		0.056	65b ₁ -72a ₂ , 64a ₂ -73b ₁		
	-0.054	69b ₁ -70a ₂ , 69b ₁ -70a ₂	19	3200611/58172	
	¹ B ₂	0.942			69b ₁ -70a ₂
0.092	68a ₂ -71b ₁				
0.195	69b ₁ -71b ₁ , 69b ₁ -70a ₂				
-0.118	69b ₁ -75a ₂ , 68a ₂ -70a ₂				
5	¹ A ₁	1.000	77b ₁ ² , 78a ₂ ⁰	12	3203365/47037
		-0.057	73a ₂ -80a ₂ , 72b ₁ -81b ₁		
		-0.057	77b ₁ -78a ₂ , 77b ₁ -78a ₂		
	-0.056	73a ₂ -81b ₁ , 72b ₁ -80a ₂	19	3200665/57773	
	¹ B ₂	0.941			77b ₁ -78a ₂
0.098	76a ₂ -79b ₁				
0.192	77b ₁ -79b ₁ , 77b ₁ -78a ₂				
-0.106	77b ₁ -83a ₂ , 76a ₂ -78a ₂				
0.081	77b ₁ -83a ₂ , 69a ₂ -78a ₂				
-0.079	77b ₁ -78a ₂ , 76a ₂ -78a ₂				
6	¹ A ₁	1.000	36b ₁ ² , 37a ₂ ⁰	13	354504/37547
		-0.073	36b ₁ -37a ₂ , 36b ₁ -37a ₂		
	-0.053	36b ₁ -38b ₁ , 36b ₁ -38b ₁	21	353626/21142	
	¹ B ₂	-0.933			36b ₁ -37a ₂
	-0.132	33b ₁ -37a ₂			
	-0.074	26b ₁ -37a ₂			
	0.203	36b ₁ -44b ₁ , 36b ₁ -37a ₂			
	-0.105	36b ₁ -38b ₁ , 36b ₁ -37a ₂			
-0.097	36b ₁ -43a ₂ , 36b ₁ -38b ₁				
-0.084	36b ₁ -38b ₁ , 30b ₁ -37a ₂				
-0.079	36b ₁ -38b ₁ , 33b ₁ -37a ₂				
7	¹ A	1.000	92b ² , 93a ⁰	17	6056526/27083
		-0.084	92b-93a, 92b-93a		
		0.068	91a-98a, 90b-97b		
		0.067	91a-97b, 90b-98a		
	-0.051	92b-94b, 88b-94b	11	6054054/70616	
	¹ B	0.940			92b-93a
	0.075	89a-95b			
	0.189	92b-93a, 89a-93a			
	-0.096	92b-93a, 86a-93a			
	0.085	92b-93a, 85a-93a			
0.070	89a-93a, 88b-93a				

TABLE 10: (Continued)

molecule	state	mixing coefficient ^{a,d}	configuration ^e	no. of configurations ^b	linked operators ^c
8	¹ A ₁	1.000	76b ₁ ² , 77a ₂ ⁰	7	3143037/48914
		-0.070	76b ₁ -77a ₂ , 76b ₁ -77a ₂		
		0.058	71b ₁ -81b ₁ , 70a ₂ -80a ₂		
	¹ B ₂	0.057	71b ₁ -80a ₂ , 70a ₂ -81b ₁	16	3140535/52480
		0.944	76b ₁ -77a ₂		
		-0.156	76b ₁ -79b ₁ , 76b ₁ -77a ₂		
		-0.127	76b ₁ -78b ₁ , 76b ₁ -77a ₂		
		0.099	76b ₁ -82a ₂ , 75a ₂ -77a ₂		
		0.091	75a ₂ -77a ₂ , 74b ₁ -77a ₂		
		-0.091	76b ₁ -77a ₂ , 75a ₂ -77a ₂		
9	¹ A ₁	1.000	84b ₁ ² , 85a ₂ ⁰	11	3143037/45781
		-0.075	84b ₁ -85a ₂ , 84b ₁ -85a ₂		
		-0.059	79b ₁ -89b ₁ , 78a ₂ -88a ₂		
		-0.059	79b ₁ -88a ₂ , 78a ₂ -89b ₁		
	¹ B ₂	0.940	84b ₁ -85a ₂	22	3140535/52903
		-0.078	83a ₂ -86b ₁		
		0.166	84b ₁ -86b ₁ , 84b ₁ -85a ₂		
		-0.114	84b ₁ -87b ₁ , 84b ₁ -85a ₂		
		0.103	84b ₁ -85a ₂ , 83a ₂ -85a ₂		
		-0.095	84b ₁ -90a ₂ , 83a ₂ -85a ₂		
		-0.092	83a ₂ -85a ₂ , 82b ₁ -85a ₂		

^a CI coefficients for the ground state are larger than 0.05, and for the excited state, they are larger than 0.07. ^b Number of configurations that have a CI coefficient larger than 0.03. ^c Linked operators total generated/selected. ^d For the SAC, by definition, the coefficient of HF configuration is always 1.00. ^e Orbital numbers and orbital symmetries along with occupation.

HLG decreases because of the increase in conjugation, the MO character has changed now. There is charge transfer kind of transition when exciting the electron from the HOMO to LUMO, which is also clear from the lack of any contribution of the donating groups in the LUMO. Thus, it becomes clearly a D-A-D type of molecule. This change in the transition character from $n = 2$ is responsible for the blue shift.

Conclusions

Although a biradical gets perturbed and becomes a biradicaloid upon substitution, the degenerate orbitals of the biradical, which are now HOMO, and the LUMO are nearly degenerate. There is tendency of the electron from the HOMO to occupy the LUMO, and this is reflected in the selected configurations where the doubly occupied LUMO configuration contributes to the ground state and the lowest-excited configuration is dominated by the HOMO-LUMO transition. Such mixing brings down the excitation energy. Studies on the variation of the bond angle C3-C2-C4 in the unsubstituted oxyallyl suggests that the absorption is basically correlated to the angle and that the HLG also reduces upon increasing the bond angle. Substitutions, which perturb the HLG and lower it but do not change the MO character, are responsible for the observed red shifts. But on the other hand, increasing the conjugation changes the character of the HOMO, and although there is reduction of the HLG, the transitions are no longer what is observed in a biradicaloid but more of a charge-transfer transition like in a D-A-D molecule. These observations, we conclude, should be helpful as design principles for these dyes.

Acknowledgment. The authors thank the Director of IICT and the Head of the Inorganic Chemistry division of IICT for their constant encouragement in this work. K.Y. and S.S. thank CSIR, India, for the JRF and SRF fellowships, respectively.

Supporting Information Available: Figures showing the one-electron molecular orbitals for molecules A-F and 1-9 and tables showing the ground to excited charge transfer of oxyallyl, the HOMO-LUMO gap, excitation energy, oscillator

strength, and dipole moments of molecules 4, 5, 8, and 9, and the charge transfer in molecules 7 and 9. This material is available free of charge via the Internet at <http://pubs.acs.org>.

References and Notes

- (1) Fabian, J. *Chem. Rev.* **1992**, 92, 1197.
- (2) Fabian, J.; Zahradnik, R. *Angew. Chem., Int. Ed. Engl.* **1989**, 28, 677.
- (3) Law, K. Y. *Chem. Rev.* **1993**, 93, 449.
- (4) *IR Absorbing Dyes*; Matsuoka, M., Ed.; Plenum Press: New York, 1990. (b) *Near-Infrared Dyes for High Technology Applications*; Daehne, S., Resch-Genger, U., Wolfbeis, O. S., Eds.; NATO ASI Series 3; Kluwer Academic: Dordrecht, The Netherlands, 1998; Vol. 52.
- (5) Tian, M.; Tatsuura, S.; Furuki, M.; Sato, Y.; Iwasa, I.; Pu, L. S. *J. Am. Chem. Soc.* **2003**, 125, 348.
- (6) Tatsuura, S.; Tian, M.; Furuki, M.; Sato, Y.; Iwasa, I.; Mitsu, H. *Appl. Phys. Lett.* **2004**, 84, 1450.
- (7) Tatsuura, S.; Mastubara, T.; Tian, M.; Mitsu, H.; Iwasa, I.; Sato, Y.; Furuki, M. *Appl. Phys. Lett.* **2004**, 85, 540.
- (8) Prabhakar, Ch.; Krishna Chaitanya, G.; Sitha, S.; Bhanuprakash, K.; Jayathiritha Rao, V. *J. Phys. Chem. A* **2005**, 109, 2614.
- (9) Langhals, H. *Angew. Chem., Int. Ed.* **2003**, 42, 4286.
- (10) Meier, H.; Dullweber, U. *J. Org. Chem.* **1997**, 62, 4821.
- (11) Meier, H.; Dullweber, U. *Tetrahedron Lett.* **1996**, 37, 1191.
- (12) Meier, H.; Petermann, R.; Gerold, J. *Chem. Comm.* **1999**, 977.
- (13) Law, K. Y. *J. Phys. Chem.* **1987**, 91, 5184.
- (14) Bigelow, R. W.; Freund, H. J. *Chem. Phys.* **1986**, 107, 159.
- (15) König, W. *J. Prakt. Chem.* **1925**, 112, 1.
- (16) Ismailsky, W. Dissertation, Universität Dresden, Dresden, Germany, 1913.
- (17) Dilthey, W.; Wizinger, R. *J. Prakt. Chem.* **1928**, 118, 321.
- (18) Wizinger, R. *Chimia* **1961**, 15, 89.
- (19) Griffiths, J. *Colour and Constitution of Organic Molecules*; Academic Press: London, 1976.
- (20) Dahne, S.; Kulpe, S. *Structural Principles of Unsaturated Organic Compounds*; Akademie Verlag: Berlin, 1977 (Abh. Akad. Wiss. DDR 8).
- (21) Dewar, M. J. S.; Dougherty, R. C. *The PMO Theory of Organic Chemistry*, 1st ed.; Plenum: New York, 1975; pp 410-418.
- (22) Simard, T. P.; Yu, J. H.; Zebrowski-Young, J. M.; Haley, N. F.; Detty, M. R. *J. Org. Chem.* **2000**, 65, 2236.
- (23) Detty, M. R.; Mckelvey, J. M.; Luss, H. R. *Organometallics* **1988**, 7, 1131.
- (24) Kim, S. H.; Hwang, S. H.; Song, H. C.; Yoon, N. S. *J. Korean Chem. Soc.* **1996**, 40, 741.
- (25) Meyers, F.; Chen, C. T.; Marder, S. R.; Bredas, J.-L. *Chem.-Eur. J.* **1997**, 3, 530.
- (26) Yang, M.; Jiang, Y. *Phys. Chem. Chem. Phys.* **2001**, 3, 4213.
- (27) Gude, C.; Rettig, W. *J. Phys. Chem. A* **2000**, 104, 8050.

- (28) Momicchioli, F.; Tatikolov, A. S.; Vanossi, D.; Ponterini, G. *Photochem. Photobiol. Sci.* **2004**, *3*, 396.
- (29) Bello, K. A.; Ajayi, J. O. *Dyes Pigm.* **1996**, *31*, 79.
- (30) Keil, D.; Hartmann, H.; Reichardt, C. *Liebigs Ann. Chem.* **1993**, *935*.
- (31) Nakjima, T.; Nakatsuji, H. *Chem. Phys. Lett.* **1997**, *280*, 79.
- (32) Wan, J.; Ehara, M.; Hada, M.; Nakatsuji, H. *J. Chem. Phys.* **2000**, *113*, 5245.
- (33) Nakajima, T.; Nakatsuji, H. *Chem. Phys. Lett.* **1999**, *300*, 1.
- (34) Wan, J.; Hada, M.; Ehara, M.; Nakatsuji, H. *J. Chem. Phys.* **2001**, *114*, 842.
- (35) Nakatsuji, H. *Acta Chim. Hung.* **1992**, *129*, 719. (b) Nakatsuji, H. In *Computational Chemistry-Reviews of Current Trends*; Leszczynski, J., Ed.; World Scientific: River Edge, NJ, 1997; Vol. 2.
- (36) Hu, Z.; Boyd, R. J.; Nakatsuji, H. *J. Am. Chem. Soc.* **2002**, *124*, 2664.
- (37) Frisch, M. J.; Trucks, G. W.; Schlegel, H. B.; Scuseria, G. E.; Robb, M. A.; Cheeseman, J. R.; Montgomery, J. A., Jr.; Vreven, T.; Kudin, K. N.; Burant, J. C.; Millam, J. M.; Iyengar, S. S.; Tomasi, J.; Barone, V.; Mennucci, B.; Cossi, M.; Scalmani, G.; Rega, N.; Petersson, G. A.; Nakatsuji, H.; Hada, M.; Ehara, M.; Toyota, K.; Fukuda, R.; Hasegawa, J.; Ishida, M.; Nakajima, T.; Honda, Y.; Kitao, O.; Nakai, H.; Klene, M.; Li, X.; Knox, J. E.; Hratchian, H. P.; Cross, J. B.; Adamo, C.; Jaramillo, J.; Gomperts, R.; Stratmann, R. E.; Yazyev, O.; Austin, A. J.; Cammi, R.; Pomelli, C.; Ochterski, J. W.; Ayala, P. Y.; Morokuma, K.; Voth, G. A.; Salvador, P.; Dannenberg, J. J.; Zakrzewski, V. G.; Dapprich, S.; Daniels, A. D.; Strain, M. C.; Farkas, O.; Malick, D. K.; Rabuck, A. D.; Raghavachari, K.; Foresman, J. B.; Ortiz, J. V.; Cui, Q.; Baboul, A. G.; Clifford, S.; Cioslowski, J.; Stefanov, B. B.; Liu, G.; Liashenko, A.; Piskorz, P.; Komaromi, I.; Martin, R. L.; Fox, D. J.; Keith, T.; Al-Laham, M. A.; Peng, C. Y.; Nanayakkara, A.; Challacombe, M.; Gill, P. M. W.; Johnson, B.; Chen, W.; Wong, M. W.; Gonzalez, C.; Pople, J. A. *Gaussian 03*, revision B.01; Gaussian, Inc.: Wallingford, CT, 2004.
- (38) Lichtenberger, D. L.; Fenske, R. F. *QCPE* **1975**, *11*, 284, (<http://qcpe.chem.indiana.edu>).
- (39) Michl, J.; Bonacic-Koutecky, V. *Tetrahedron* **1988**, *44*, 7559.
- (40) Hrovat, D. A.; Murcko, M. A.; Lahti, T. M.; Borden, W. T. *J. Chem. Soc., Perkin Trans. 2* **1998**, 1037.
- (41) Reed, A. E.; Weinstock, R. B.; Weinhold, F. *J. Chem. Phys.* **1985**, *83*, 735. (b) Reed, A. E.; Weinhold, F.; Curtiss, L. A. *Chem. Rev.* **1988**, *88*, 899. (c) Glendening, E. D.; Reed, A. E.; Carpenter, J. E.; Weinhold, F. *NBO*, version 3.1; Theoretical Chemistry Institute, University of Wisconsin: Madison, WI.
- (42) Detty, M. R.; Henne, B. *Heterocycles* **1993**, *35*, 1149.
- (43) Neuse, E. W.; Green, B. R. *J. Am. Chem. Soc.* **1975**, *97*, 3987.